Table V. Least-Squares Planes[a] and Atomic Deviations (Å) Therefrom for $InCl[(CH_3)_2NCH_2C_6H_4)]_2$

(a) $-0.3819X - 0.5685Y - 0.7287Z = -7.0518$
In, 0.006; Cl, −0.001; C(11), −0.003; C(21), −0.003

(b) $0.0166X + 0.5947Y - 0.8038Z = -3.9983$
In, 0.020; Cl, 0.001; N(1), −0.010; N(2), −0.010

(c) $0.7279X - 0.3787Y - 0.5716Z = -2.9407$[b]
C(11), −0.002; C(12), 0.001; C(13), 0.001; C(14), 0.001; C(15), 0.002; C(16), 0.002

(d) $-0.9776X + 0.1582Y - 0.1389Z = -3.1048$[b]
C(21), −0.008; C(22), 0.003; C(23), 0.007; C(24), −0.011; C(25), 0.006; C(26), 0.003

[a] Dihedral angles: between planes a and b, 76.0°; between planes c and d, 134°. [b] In atom is 0.080 Å from plane c and 0.281 Å from plane d.

$H_3)_2InCl]_2$, which is described as a distorted octahedron[28] but may perhaps be better viewed as a distorted trigonal bipyramid.

The In–C bond lengths of 2.144 (3) and 2.154 (3) Å compare well with the In–C(aryl) values of 2.111 (14) and 2.155 (14) Å found in $(C_6H_5)_3In$,[13] the sum of the covalent radii being 2.21 Å. Similar values have been observed in alkylindium compounds (2.179 (7) Å in $[(CH_3)_2InCl]_2$,[28] 2.17 Å (average) in $(CH_3)_2InBr$,[29] 2.08 (1) and 2.11 (1) Å in $(CH_3)_2InOAc$,[30] 2.14 Å in $(C_2H_5)_2InOSCH_3$,[31] and 2.16 (2) Å (average) in $[(CH_3)_2In(ON{=}CHC_5H_4N)]_2$[15]). The In–C bond lengths in $[CH_3InCl_2]_2$ (2.052 (9) Å),[16] $(C_2H_5)_2InOAc$ (2.22 and 2.29 Å),[32] and $[In(CH_3)_4]^-$ (2.239 (3), 2.26 (2) Å)[33] fall outside the range of 2.10–2.18 Å derived from the above group of compounds.

There is only a limited amount of information from X-ray studies on In–N bond lengths. In the distorted TBP complex $[(CH_3)_2In(ON{=}CHC_5H_4N)]_2$, the oximate nitrogen atoms form In–N bonds in an equatorial plane of a length (2.271 (16) and 2.288 (15) Å)[15] almost identical with the values for octahedral $[InCl_2(acac)(bpy)]$ (2.276 (4) and 2.299 (4) Å)[27] and very close to those in $InCl_3$·terpy (2.238 (3), 2.268 (3), 2.281 (3) Å).[26] The sum of the covalent radii is 2.19 Å. The present values of 2.442 (3) and 2.482 (2) Å for the two axial In–N bonds in L_2InCl are substantially greater than the "normal" value of ~2.28 Å for an In–N single bond (vide supra) but come close to the only other reported value for axial In–N bonds in a TBP complex, namely, 2.501 (17) and 2.514 (19) Å for the In–N bonds formed by the pyridine nitrogen atoms in $[(CH_3)_2In(ON{=}CHC_5H_4N)]_2$.[15] There are a number of possible reasons for these differences. The apical bonds in TBP complexes are generally weaker than those in the equatorial plane,[20] a diorganoindium chloride will have weaker acceptor properties than $(acac)InCl_2$ or $InCl_3$, and, finally, the skeletal strain in the five-membered chelate rings will contribute to the weakening of the In–N bond (cf. a similar lengthening of the Sn–N bond in $(C_6H_5)_2LSnBr$[21]).

Acknowledgment. This work was supported by grants from the Natural Sciences and Engineering Research Council of Canada and from the North Atlantic Treaty Organization. We thank Professor Milton Glick (Wayne State University) for helpful discussions and for hospitality to P.W.R.C. during a sabbatical leave.

Registry No. L_2InCl, 74552-66-2.

Supplementary Material Available: A table of observed and calculated structure factor amplitudes (9 pages). Ordering information is given on any current masthead page.

(28) Hausen, H. D.; Mertz, K.; Veigel, E.; Weidlein, J. *Z. Anorg. Allg. Chem.* **1974**, *410*, 156.
(29) Hausen, H. D.; Mertz, K.; Weidlein, J.; Schwartz, W. *J. Organomet. Chem.* **1975**, *93*, 291.
(30) Einstein, F. W. B.; Gilbert, M. M.; Tuck, D. G. *J. Chem. Soc., Dalton Trans.* **1973**, 248.
(31) Hausen, H. D. *Z. Naturforsch., B: Anorg. Chem., Org. Chem., Biochem., Biophys., Biol.* **1972**, *27B*, 82.
(32) Hausen, H. D. *J. Organomet. Chem.* **1972**, *39*, C37.
(33) Hoffman, K.; Weiss, E. *J. Organomet. Chem.* **1973**, *50*, 17.

Contribution from the Department of Chemistry, Rutgers—The State University, New Brunswick, New Jersey 08903

Synthesis, Hyperfine Interactions, and Lattice Dynamics of the Intercalation Compounds $FeOCl[(CH_3O)_3P]_{1/6}$ and $FeOCl[(CH_3CH_2)_3P]_{1/6}$

R. H. HERBER* and Y. MAEDA[1]

Received March 20, 1980

Trimethyl phosphite (TMP) and triethylphosphine (TEP) have been intercalated into FeOCl to give layer compounds in which half of the "guest" molecule sites in the van der Waals layer are occupied. Intercalation causes a major expansion in the *b*-axis direction of the FeOCl lattice, and room-temperature X-ray powder pattern data show this expansion to correspond to 6.47 and 3.96 Å, respectively. Detailed temperature-dependent ^{57}Fe Mössbauer experiments over the range $4.2 \leq T \leq 320$ K have shown that there are two different iron atoms in the intercalate corresponding to those Fe atoms which have a "guest" molecule nearest neighbor ($^1/_6$) and those iron atoms which are more distant from the intercalant Lewis base unshared electron pair. The magnetic hyperfine field at liquid-helium temperature is essentially unchanged from that observed in unintercalated FeOCl. The isomer shift and and quadrupole splitting data show a discontinuity at ~220 K, from which it is inferred that the energetics of "guest" molecule binding in the van der Waals layer is on the order of 0.7 kcal mol^{-1}. Fourier-transform infrared spectra of the intercalant show that a number of the fundamental molecular vibrational modes are inhibited when the guest molecule resides in the host lattice and that significant spectral changes in the C–P region occur on sample cooling, again suggesting a direct interaction between the lone-pair electrons of the phosphorus atom and the FeOCl lattice.

Introduction

FeOCl is a layered compound belonging to the orthorhombic space group *Pmnm* (D_{2h}^{13}) with two formula units per unit cell. The crystal structure was initially determined by Goldztaub[2a] and more recently refined by Lind.[2b] The unit cell dimensions are $a = 3.780$, $b = 7.917$, and $c = 3.302$ Å. The crystal structure consists of a stack of double layer sheets of *cis*-

(1) Permanent address: Department of Chemistry, Faculty of Science, Kyushu University, Hakozaki, Fukuoka, Japan.

(2) (a) Goldsztaub, S. *C. R. Hebd. Seances Acad. Sci.* **1934**, *198*, 667; *Bull. Soc. Fr. Mineral.* **1935**, *58*, 6. (b) Lind, M. D. *Acta Crystallogr. Sect. B* **1970**, *B26*, 1058.

0020-1669/80/1319-3411$01.00/0

$FeCl_2O_4$ octahedra linked together with shared edges. Of particular significance is the fact that the chlorine atoms lie on a plane which defines the edge of each layer, and the bonding across these chlorine atom planes is assumed to be of the van der Waals type. The van der Waals interaction is readily disrupted, and the intercalation of a wide variety of amine bases (including NH_3 itself) has been observed to occur under relatively mild conditions.[3,4] The orientation of the intercalated molecular species has been the subject of extensive study,[5-7] and the *b*-axis expansion of the unit cell as derived from X-ray powder pattern data has been used to elucidate the steric relationships between the guest molecule and the host lattice.

Although a large number of different amine bases—including ammonia, pyridine,[5,8,9] 2,6-dimethylpyridine,[8] 4-aminopyridine,[8] and 2,4,6-trimethylpyridine[8]—have been successfully intercalated into FeOCl, Lewis base guest molecules not containing nitrogen atoms have so far not been examined. Indeed it has been observed that while nonstoichiometric iron(III) oxychloride is capable of intercalating a large number of molecules having Lewis base character, stoichiometric FeOCl base intercalations have so far been restricted to pyridine and its derivatives. A lithium intercalate, $FeOCl{\cdot}Li_x$ ($x < 0.50$), has been reported by Palvadeau et al.[4] The FeOCl intercalation of two cyclopentadienyl organometallic compounds has been reported by Halbert et al.[10]

In the present study, the first examples of phosphorus-containing Lewis bases have been examined as guest molecules in an FeOCl host matrix, and the hyperfine interactions, lattice dynamics, and vibrational spectra of FeOCl(TMP) and FeOCl(TEP) are discussed in detail.

Experimental Section

(a) Sample Preparation. Iron(III) oxychloride was prepared from Fe_2O_3 and $FeCl_3$ by the usual sealed-tube technique discussed in the literature.[5,8,9] The optimal conditions were found to be a 1-week heating period in a temperature gradient of ~70 °C at a mean temperature of 385 °C. The dark red-violet bladelike crystals which grow at the cool end of the reaction tube were removed free of unreacted starting material and stored under nitrogen at room temperature. reaction yield under these conditions is estimated to be ~50%. the TEP intercalate was obtained by soaking FeOCl in a 2-propanol solution of triethylphosphine for 24 days at 40 °C. At the end of the reaction period, the reaction mixture was filtered through sintered glass, and then the solid product was washed with absolute alcohol, dried in vacuo, and stored under nitrogen. Anal. Calcd for $FeOCl[(C_2H_5)_3P]_{1/6}$: Fe, 43.98; C, 9.45; H, 1.97; Cl, 27.92; P, 4.07. Found: Fe, 43.78; C, 8.34; H, 2.18; Cl, 25.45; P, 3.67. The observed Fe:P ratio is 6.6:1 in modest agreement with the indicated stoichiometry. The departure of this ratio from the ideal value of 6:1 arises from crystal-surface effects which reduce the number of "guest" molecules intercalated per iron atom near the edge of the crystal. This point will be more fully discussed below. The TMP intercalate was obtained similarly, except that reaction was judged to be complete in ~19 h at 40 °C. Anal. Calcd for $FeOCl[(OCH_3)_3P]_{1/6}$: Fe, 43.64; C, 4.69; H, 1.17; Cl, 27.70; P, 4.05. Found: Fe, 44.08; C, 4.05; H, 1.04; Cl, 27.89; P, 3.44. The observed Fe:P ratio is 7.1:1. As Hagenmuller et al.[3] and others have pointed out, the stoichiometry of the FeOCl intercalates is strongly dependent on the steric requirements of the Lewis base "guest" atom, and the FeOCl:G (where G is the intercalant species) ratio of 6:1 appears to represent the limiting stoichiometry when G is a phosphine or phosphite base. Efforts to prepare intercalation systems with a higher phosphine base to FeOCl ratio have so far not been successful.

(b) ^{57}Fe Mössbauer Spectroscopy. Nuclear γ resonance spectroscopy was effected by using a constant-acceleration spectrometer as described earlier.[11,12] Velocity calibration is based on the magnetic hyperfine spectrum of 0.8-mil NBS SRM iron foil at 295 K, and all isomer shifts are reported with respect to the centroid of this spectrum. Temperature control to better than ±0.1 K over the time intervals needed for spectral data accumulation (usually 4–20 h) was achieved with the use of a proportional controller to drive the heater circuit of an Air Products Heli-tran cryostat. Data reduction was effected by using a matrix-inversion least-squares routine on the Rutgers University IBM 370/68 computer.

(c) Fourier-Transform Infrared Spectroscopy. Room-temperature spectra were obtained on 0.3–0.6% by weight samples in KBr, with a Nicolet 7000 spectrometer[13] over the range 4000–400 cm^{-1}. The sample chamber was thoroughly purged with boil-off N_2 prior to data accumulation.

Results and Discussion

(a) Lattice Parameters of Intercalated FeOCl. Using elemental analysis for C, H, P, and Cl as well as a colorimetric procedure for iron, it was possible to establish the stoichiometry of both intercalate systems to correspond to one base molecule to six FeOCl formula units. The X-ray powder patterns of these solids show that while the *a*- and *c*-axis parameters do not change significantly when FeOCl is intercalated with a "guest" molecule, the *b*-axis parameter undergoes a large expansion which is readily determined from the positions of the (010) and (020) peaks. For unintercalated FeOCl, the *b*-axis unit-cell dimension is 7.91 ± 0.01 Å. This value increases to 11.87 ± 0.02 Å for the TEP intercalate and to 14.38 ± 0.02 Å for the TMP intercalate. It is interesting to note that the latter value is almost that of the largest *b*-axis expansion so far observed, i.e., $FeOCl(2,6\text{-lut})_{1/6}$ for which the *b*-axis dimension is 14.80 ± 0.02 Å.

Before turning to the question of the orientation of the intercalated "guest" molecule relative to the symmetry of the FeOCl structure, it is appropriate to consider the relationship between the location of the intercalant and the stoichiometry observed for these compounds. It is clear from a wide variety of evidence that the intercalant occupies a position in the van der Waals layer. Two adjacent layers form sites in which three chlorine atoms (two from one layer and one from the adjacent layer) are oriented toward each other. If the "guest" molecule is sufficiently small (e.g., NH_3, C_5H_5N, etc.) each of these sites can be occupied by such a "guest" and the limiting Fe:G ratio will be 3:1. For larger intercalant molecular species only a fraction of these sites will be occupied and the limiting Fe:G ratio will consequently become larger. For the TEP and TMP intercalates it is clear from the stoichiometry that every other interlayer site in the bulk matrix can be occupied and thus the limiting Fe:G (in this case G is the phosphorus-containing Lewis base and hence is experimentally obtained from the P elemental analysis data) ratio will be 6:1. The observation that the experimental value of this ratio is somewhat greater than this (see above) can be rationalized on the basis that the FeOCl moieties located near the edge of the crystals will not be able to form appropriate sites and thus will not be able to

(3) Hagenmuller, P.; Portier, J.; Barbe, B.; Bouclier, P. *Z. Anorg. Allg. Chem.* **1967**, *355*, 209.
(4) Palvadeau, P.; Coic, L.; Rouxel, J.; Portier, J. *Mater. Res. Bull.* **1978**, *13*, 221.
(5) Kanamaru, F.; Yamanaka, S.; Koizumi, M.; Nagai, S. *Chem. Lett.* **1974**, 373.
(6) Yamanaka, S.; Nagashima, T.; Tanaka, M. *Thermochim. Acta* **1977**, *19*, 236.
(7) Schöllhorn, R.; Zagefka, H. D.; Butz, T.; Lerf, A. *Mater. Res. Bull.* **1979**, *14*, 369. Riekel, C.; Hohlwein, D.; Schöllhorn, R. *J. Chem. Soc., Chem. Commun.* **1976**, 863.
(8) Kikkawa, S.; Kanamaru, F.; Koizumi, M. *Bull. Chem. Soc. Jpn.* **1979**, *52*, 963.
(9) Kanamaru, F.; Shimada, M.; Koizumia, M.; Takano, M.; Takada, T. *J. Solid State Chem.* **1973**, *7*, 297.
(10) Halbert, T. R.; Thompson, A. H.; McCandlish, L. E. *Physica B+C (Amsterdam)* **1980**, *99B+C*, 128. Halbert, T. R.; Scanlon, J. *Mater. Res. Bull.* **1979**, *14*, 415.
(11) Herber, R. H.; Maeda, Y. *Physica B+C (Amsterdam)* **1980**, *99B+C*, 352 and references therein.
(12) Rein, A. J.; Herber, R. H. *J. Chem. Phys.* **1975**, *63*, 1021 and references therein.
(13) Merck Sharp and Dohme Laboratories, Rahway, NJ.

bind the guest molecules in the structure. A similar qualitative argument can be used for crystal edges in which adjacent layers form a "step" pattern in the *b*-axis direction. Again, FeOCl units close to such an edge will not be able to form sites for the "guest" molecules, and hence the Fe:G ratio will be somewhat larger than that corresponding to the occupation of every other site. Finally it should be noted that, on the basis of the above model, the departure from the Fe:G ratio should be larger for small crystals (having a larger surface-to-volume ratio) than for large crystals. This expectation is indeed borne out experimentally and will be discussed elsewhere.[14]

Within the interlayer site referred to above, there are several possible orientations which a noncubic symmetry intercalant molecule can adopt with respect to the symmetry of the lattice. In particular, it is of interest to ascertain the orientation of the nitrogen or phosphorus lone-pair electrons with respect to the van der Waals layer, since any discussion of the "guest–host" chemical interaction must take this question into account.

Since the low molecular weight trialkylphosphines and trialkyl phosphites are liquids at room temperature, there are no single-crystal X-ray diffraction data available as a guide to the molecular size of these molecules. However, a reasonable approximation to these parameters can be extracted from the diffraction data for the related phosphine sulfides and selenides. The structure of $(C_2H_5)_3PS$ has been discussed by van Meerssche and Lêonard,[15] who showed that the distance from the phosphorus nucleus to the methyl carbon is approximately 2.15 Å. Assuming a normal covalent radius for the CH_3 hydrogen and approximately tetrahedral geometry for $(C_2H_5)_3P$ (with the lone pair occupying the fourth vertex) leads to a molecular diameter normal to the C_{3v} axis of ~3.9 Å. In contrast the molecular diameter parallel to this symmetry axis can be estimated to be ~2.5 Å from the crystallographic data on the sulfide and selenide.[15,16] Since the *b*-axis expansion in the TEP intercalation compound is ~3.96 Å, the present data lend strong support to the observation that, within the FeOCl matrix, the orientation of the "guest" molecule is such that the phosphorus atom lone pair is directed parallel to the van der Waals plane defined by the chlorine atoms in the layer structure.

In the case of the TMP intercalation compound, the *b*-axis expansion was determined to be 6.47 Å and is a reflection of the more nearly linear C–O–P conformation in TMP compared to the nearly tetrahedral C–C–P bond angle in TEP, presumably due to the mutual repulsion of the two nonbonding electron pairs on the oxygen atom in the former.

These structural inferences are at variance with the model suggested by Kanamaru et al.[5,9] for the pyridine intercalate of iron oxychloride. These authors have examined the system $FeOCl(C_5H_5N)_{1/3}$ in some detail and concluded, from the change in the *b*-axis parameter as well as from a one-dimensional electron density projection (on the *b* axis) using nine (00*l*) reflections observed in the powder pattern X-ray data, that the pyridine lone-pair electrons are oriented toward the chlorine atoms. In their model the pyridine molecules are oriented in an alternating array with the twofold axis parallel to the O–Fe–Cl bond axis.

(b) Recoil-Free Fractions and Lattice Temperatures. At temperatures well above the magnetic ordering temperature, the temperature dependence of the area under the resonance curve can be used to estimate a "lattice temperature", Θ_M, on the basis of the thermal motion of the Mössbauer active atom. The temperature dependence of the (normalized) area is

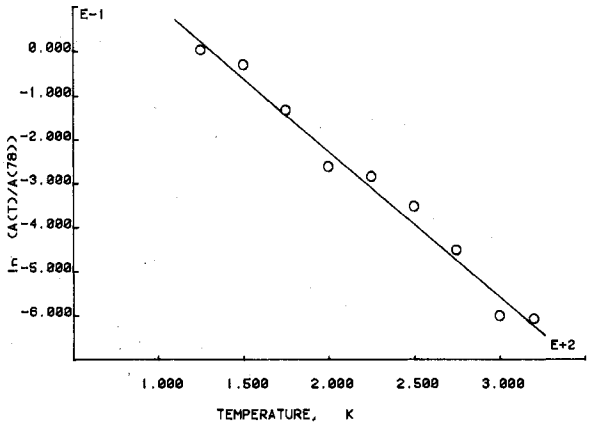

Figure 1. Temperature dependence of the area under the ^{57}Fe Mössbauer resonance curve for the TEP intercalate in the range 125 ≤ *T* ≤ 320 K.

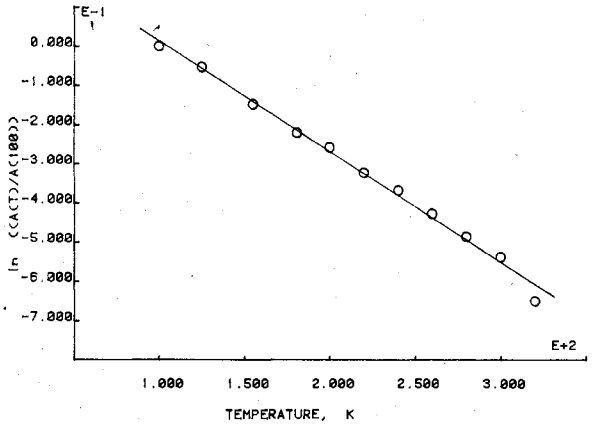

Figure 2. Temperature dependence of the area under the ^{57}Fe Mössbauer resonance curve for the TMP intercalate in the range 100 ≤ *T* ≤ 320 K.

summarized for the TEP intercalate in Figure 1 and for the TMP intercalate in Figure 2. As noted previously[11] in the case of ^{57}Fe Mössbauer data, two "lattice temperatures" can be calculated from such data. Using a Debye model for the solid and assuming that the appropriate mass of the probe corresponds to the free-atom value lead[11] to a temperature dependence of the recoil-free fraction, *f*, given by

$$\mathrm{d} \ln f/\mathrm{d}T = -6E_R/k_B\Theta_M^2 \qquad (1)$$

in which E_R is the recoil energy after γ-ray emission and k_B is Boltzmann's constant. Equation 1 can be replaced for a thin absorber by the temperature dependence of the area under the resonance curve (appropriately normalized) and finally yields

$$\Theta_M = \frac{E\gamma}{c}\left[\frac{-3}{M_{eff}k_B\,\mathrm{d} \ln [A(T)/A(78)]/\mathrm{d}T}\right]^{1/2} \qquad (2)$$

For ^{57}Fe this equation reduces to

$$\Theta_M = 11.659\left[\frac{-\mathrm{d} \ln [A(T)/A(78)]}{\mathrm{d}T}\right]^{-1/2} \qquad (3)$$

A limitation of this approach is that when the Mössbauer-active atom is incorporated in the solid by largely covalent bonding forces, the appropriate mass needed to describe the motional behavior may be significantly larger than the atomic mass. This "effective mass" description has been especially successful in the case of molecular solids, such as the organometallic compounds of iron[17] and tin.[12,18] In the case

(14) Herber, R. H.; Maeda, Y., unpublished results on the kinetics of amine intercalation into FeOCl. These data will be published in connection with a detailed study of the system FeOCl(py).
(15) van Meerssche, M.; Lêonard, A. *Bull. Soc. Chim. Belg.* **1959**, *68*, 683.
(16) van Meerssche, M. *Bull. Cl. Sci., Acad. R. Belg.* **1954**, *40*, 846.

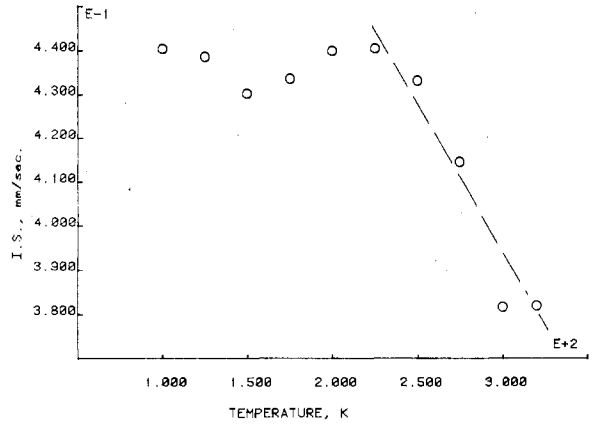

Figure 3. Temperature dependence of the isomer shift parameter for the TEP intercalate. The dashed line at high temperatures represents the "bare atom" limiting slope, $-3kT/2mc^2$. The parameter analysis is based on a two-Lorentzian fit to the data; see text.

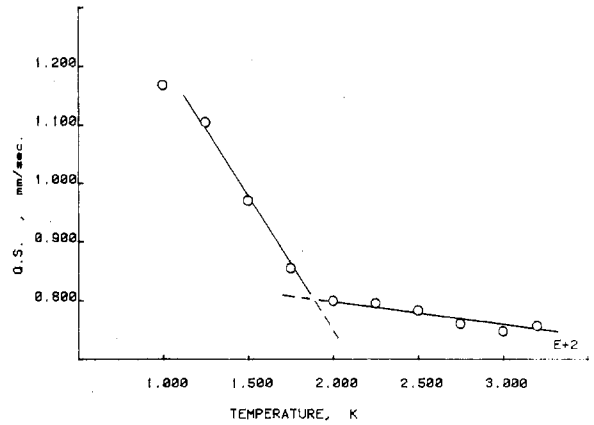

Figure 4. Temperature dependence of the quadrupole splitting parameter for the TEP intercalate in the range $100 \leq T \leq 320$ K. The parameter analysis is based on a two-Lorentzian fit to the data; see text.

of ^{57}Fe spectroscopy due to the lighter mass of the Mössbauer atom and the narrower line widths, the effective vibrating mass can frequently be estimated from the second-order Doppler shift (the temperature dependence of the isomer shift parameter) and is given by

$$M_{\text{eff}} = 4.1684 \times 10^{-2}[\text{d(IS)}/\text{d}T]^{-1} \quad (4)$$

Using this value for M_{eff} in (2) leads to a modified lattice temperature

$$\Theta_M' = 4.3203 \times 10^2 \left[\frac{-\text{d(IS)}/\text{d}T}{\text{d ln } [A(T)/A(78)]/\text{d}T} \right]^{1/2} \quad (5)$$

As will be discussed below, the isomer shift observed for the two intercalates shows a readily observable temperature discontinuity at ~220 K. In the case of the TEP intercalate, the data below this temperature cannot be fitted by a linear-regression function, although this is possible for the data obtained for the TMP intercalate, and only the high-temperature ($T \geq 250$ K) data were used to estimate the value of M_{eff} from (4). In the case of the TEP intercalate, the effective vibrating mass calculated from these data is 59 ± 2 mass units, in good agreement with the free-atom value of 56.95 for ^{57}Fe spectral data, and indicates that the effective mass corresponds to that of the bare-atom value. For the TMP intercalate, the corresponding value is 70 ± 1 mass units, a value ~20% higher than that corresponding to a "free" iron atom.

From (5), the value of Θ_M' for the TEP intercalate is calculated to be 213 ± 2 K and, as expected from the above masses, is in good agreement with the value of $\Theta = 203 \pm 2$ K calculated from (3) by using the recoil-free fraction data over the entire temperature range ($T_N < T \leq 320$ K). For the TMP intercalate, $\Theta_M = 219 \pm 1$ K, but Θ_M', calculated from (5) by using the high-temperature slope d(IS)/dT, is 198 ± 1 K, in good agreement with the value observed for the TEP intercalate also obtained by using the high-temperature d(IS)/dT data.

Inspection of the data summarized in Figures 1 and 2 shows that ln $[A(T)/A(78)]$ in the region above the magnetic ordering temperature is reasonably well fitted by a linear regression; the correlation coefficients are better than 0.991.

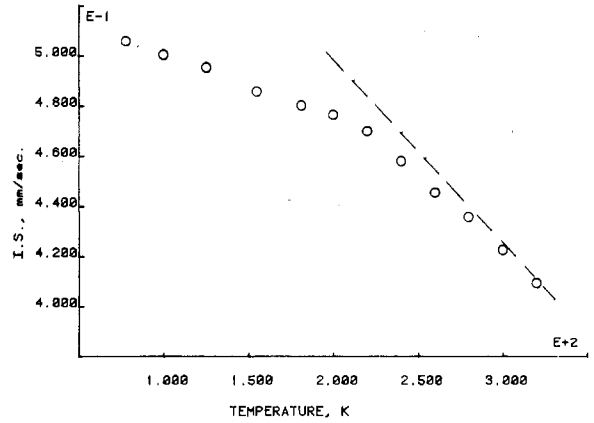

Figure 5. Temperature dependence of the isomer shift parameter for the TMP intercalate. The dashed line at high temperatures represents the "bare atom" limiting slope, $-3kT/2mc^2$. The parameter analysis is based on a two-Lorentzian fit to the data; see text.

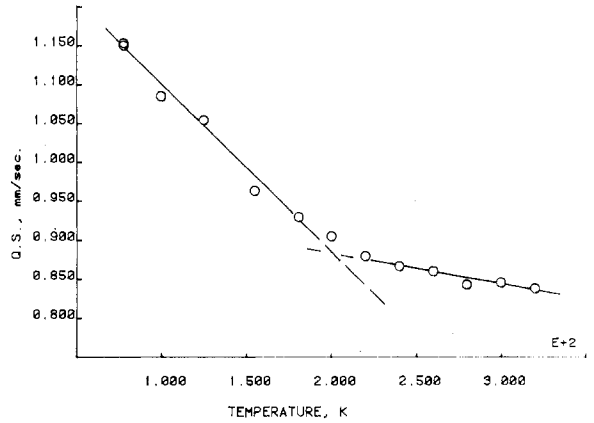

Figure 6. Temperature dependence of the quadrupole splitting parameter for the TMP intercalate in the range $78 \leq T \leq 320$ K. The parameter analysis is based on a two-Lorentzian fit to the data; see text.

Thus, there is no indication from these data of a first-order transition phase in the temperature range $100 \leq T \leq 320$ K. Indication of a transition effecting the interaction between the iron atom and its nearest neighbors is, however, evident from the temperature dependence of the isomer shift and of the quadrupole splitting parameters. These data are summarized in Figures 3–6 for the two intercalates. The isomer shift parameter for the TEP intercalate (Figure 3) is nearly inde-

(17) See, for example: Hazony, Y.; Herber, R. H. *J. Phys. (Orsay, Fr.)* **1974**, *C6*, 131. Herber, R. H.; Fischer, J. *Can. J. Spectrosc.* **1974**, *19*, 21.

(18) Herber, R. H.; Leahy, M. F. *J. Chem. Phys.* **1977**, *67*, 2718.

pendent of temperature in the range $78 \leq T \leq 150$ K. At temperatures above ~225 K the isomer shift shows a strong temperature dependence, with a slope, $d(IS)/dT$, of $-(8.1 \pm 0.5) \times 10^{-4}$ mm s^{-1} K^{-1} (based, however, on only four data points), which is close to the classical limiting slope value (-7.30×10^{-4} mm s^{-1} K^{-1}) shown in Figure 3 as a dashed line. Thermal-cycling experiments have shown that the observed temperature dependence is completely reversible on a time scale short compared to the Mössbauer data acquisition times, i.e., less than ~30 min at ~150 K.

For the TMP intercalate, the temperature dependence of the isomer shift, summarized in Figure 5, again shows a discontinuity at ~218 K. The low-temperature data ($78 \leq T \leq 200$ K) in this case can be fit by a linear regression and yield an M_{eff} from (4) of 167 ± 1 mass units and a Θ_M' from (5) of 130 K. The data above 220 K show a slope, $d(IS)/dT$, of -5.98×10^{-4} mm s^{-1} K^{-1}, somewhat smaller than the classical "bare-atom" value, which is again indicated in the figure.

A similar temperature dependence is to be noted in the quadrupole splitting (QS) data which are summarized in Figures 4 and 6. For both intercalates, the temperature dependence, $d(QS)/dT$, above 220 K is approximately 6×10^{-4} mm s^{-1} K^{-1}, which is only slightly larger than that observed for unintercalated FeOCl, for which this parameter is ~1×10^{-4} mm s^{-1} K^{-1}. In the region below 200 K, $d(QS)/dT$ is ~3.5×10^{-3} mm s^{-1} K^{-1}, but the present data are not sufficient to confirm that this temperature dependence is a sensitive function of the structure of the "guest" molecule. It should, however, be noted that in the temperature range $78 \leq T \leq 200$ K, the absolute value of the quadrupole hyperfine interaction ranges from a value ~0.27 mm s^{-1} larger than that for FeOCl at 78 K to ~0.12 mm s^{-1} smaller than that for FeOCl at 200 K.

In their study on $FeOCl(py)_{1/3}$, Kanamaru et al.[5] observed no difference in the QS parameter between the intercalate and the neat lattice but did observe a decrease of ~0.26 mm s^{-1} on intercalation in the case of $FeOCl(py)_{1/4}$.[8] It seems clear from other data[16] on amine intercalations into FeOCl that both increases and decreases in QS (300 K) can be observed and appear to be dependent both on the nature of the intercalant and on the stoichiometry of the intercalate. The decrease in QS (300 K) for the TEP and TMP intercalates is the largest so far observed in the FeOCl system.

Finally, in the context of the present discussion, it is appropriate to note that the QS parameter for both intercalates is larger than that observed for unintercalated FeOCl at liquid-nitrogen temperature and smaller than the corresponding value at 300 K. This observation is related to the bonding interaction between the "guest" molecules and the FeOCl lattice—particularly the electron density in the chlorine atom layer which defines the edge of the van der Waals gap—as will be discussed in more detail below.

The above results pertaining to the temperature dependence of the hyperfine parameters can be understood in terms of the motional degrees of freedom of the "guest" molecules in the layer structure of the intercalated FeOCl. At temperatures below ~200 K, the interaction between the intercalated molecule and the atom in the van der Waals layers is sufficiently large compared to k_BT (the mean thermal excitation energy) that the entire lattice can be considered to be a three-dimensional solid. When the temperature is raised from 78 to ~200 K, the normal three-dimensional thermal expansion causes a change in the quadrupole hyperfine interaction due to the displacement of some of the nearest-neighbor atoms relative to the iron atom. In this temperature region, the bonding across the van der Waals layer due to the presence of the "guest" molecules is sufficiently strong to be observed as a temperature-dependent decrease in QS. Above ~200 K, the bonding across the van der Waals layers becomes relatively "soft", and further atomic displacements of the atoms bonded to the iron atom due to the increase in thermal energy occur primarily in the a–c plane. Hence, at the higher temperatures, the temperature dependence of the quadrupole hyperfine interaction corresponds reasonably well to that observed for unintercalated FeOCl.

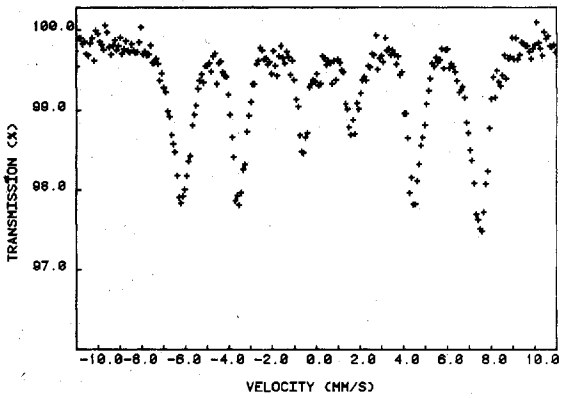

Figure 7. Mössbauer spectrum (^{57}Fe) for the TEP intercalate at 4.2 K. The resonance maxima are numbered sequentially from left to right (see text).

This model also accounts for the temperature dependence of the isomer shift at temperatures above ~200 K as already noted. At temperatures below ~200 K, where a relatively rigid three-dimensional solid structure is envisioned due to bonding across the van der Waals gap, a much smaller temperature dependence of the IS parameter is implied by this model, in agreement with the experimental data summarized in Figures 3 and 5. Finally, in this context, it should be noted that for both intercalates the linear decrease of $\ln [A(T)/A(78)]$ with temperature over the entire range ($78 \leq T \leq 320$ K) suggests that the phonon interaction with the iron atom is not sensitive to the onset of softening of the bonding across the van der Waals gap but rather reflects an averaging over all of the vibrational motions of the lattice in which the metal atom participates.

(c) Sign of the Electric Field Gradient (EFG) in the Intercalates. The most detailed study of the electric field gradient in FeOCl is that by Grant et al.[19] in which the three components of the EFG (V_{xx}, V_{yy}, and V_{zz}) as well as the asymmetry parameter were determined from Mössbauer measurements on a single-crystal sample at 23 ± 1 °C. Because the magnitude of the nuclear quadrupole moment, which must be assumed (0.33 b) in fitting the data by a self-consistent monopole–point dipole model calculation, is not in good agreement with the normally accepted value (0.19 b), the results of Grant et al.[19] have been reexamined by Sengupta, Artman, and Sawatzky.[20] These authors evaluated the overlap contributions to the EFG components in FeOCl by using a "simplified" Sawatzky formulation[21] and were able to account for the experimentally observed asymmetry parameter and a value of 0.19 b for Q (^{57}Fe). Both the Grant et al.[19] analysis and the Sengupta et al.[20] recalculation show that in unintercalated FeOCl, V_{zz}, the principal element of the symmetric second-rank EFG tensor, is negative.

Due to the nonvanishing electric field gradient at the iron nucleus in FeOCl, it is possible to determine the sign of the

(19) Grant, R. W.; Wiedersich, H.; Housley, R. M.; Espinosa, G. P.; Artman, J. O. *Phys. Rev. B: Solid State* **1971**, *3*, 678.
(20) Sengupta, D.; Artman, J. O.; Sawatzky, G. A. *Phys. Rev. B: Solid State* **1971**, *4*, 1484.
(21) Sawatzky, G. A.; Hopkes, J. *Phys. Rev. Lett.* **1970**, *25*, 100.
(22) Grant, R. W. *J. Appl. Phys.* **1971**, *42*, 1619.

Table I. Summary of ^{57}Fe Mössbauer Data for FeOCl and the TEP and TMP Intercalates[a]

	FeOCl	$FeOCl(TEP)_{1/6}$	$FeOCl(TMP)_{1/6}$
IS (78 K)[c]	0.511 ± 0.008[b]	0.447 ± 0.074	0.506 ± 0.036
IS (300 K)[c]	0.389 ± 0.006	0.382 ± 0.101	0.423 ± 0.040
d(IS)/dT[h]	-5.496×10^{-4}	-8.047×10^{-4}	-5.983×10^{-4}
QS (78 K)[c]	0.929 ± 0.010[b]	1.194 ± 0.025	1.153 ± 0.009
QS (300 K)[c]	0.917 ± 0.010	0.747 ± 0.011	0.846 ± 0.007
d ln $[[A(T)/A(78)]/dT]$[d]	-1.901×10^{-3}	-3.299×10^{-3}	-2.827×10^{-3}
M_{eff}[e]	76 ± 2	59 ± 2	167 ± 1 (78-220 K), 70 ± 1 (220-320 K)
Θ_M[f]	267 ± 5	203 ± 2	219 ± 1
$\Theta_{M,f}$	232 ± 5	213 ± 9	129 ± 1 (78-220 K), 199 ± 1 (220-320 K)
H_{eff} (4.2 K)[g]	432.2 ± 1.0	434.5 ± 0.9	431.2 ± 0.1

[a] The isomer shift scale is with reference to Fe(0) at 295 K using the same source as employed in the data runs. V_{zz} is negative for all compounds. [b] Value calculated by extrapolating data above the magnetic ordering temperature to 78 K. [c] Values given in mm s^{-1}. [d] Values given in K^{-1}. [e] Values given in mass units. [f] Values given in K. [g] Values given in kOe. [h] Values given in mm s^{-1} K^{-1}.

EFG tensor from the ^{57}Fe Mössbauer spectrum obtained at temperatures below that at which magnetic ordering occurs. A typical spectrum of the TEP intercalation compound at 4.2 K is shown in Figure 7. From the relative separation of the 1,2 and 5,6 resonance maxima, the signs of the EFG tensors in both the TEP and TMP intercalates are observed to be negative, as it is in unintercalated FeOCl, but opposite to that found in the intercalation compounds $FeOCl(py)_{1/3}$ and $FeOCl(NH_3)_{3/4}$, inter alia.[14] The specific relationship between the sign of the EFG tensor in the FeOCl intercalation compounds and the structure of the "guest" molecule has not yet been clearly established. In fact, the present evidence suggests that for intercalation compounds represented by the general formula $FeOCl(G)_n$, where G represents one molecule of the "guest" species, if $n \leq 1/4$, the sign of the EFG tensor at the iron nucleus will be negative. On the other hand if $n \geq 1/3$, this sign will be positive. Further tests of this working hypothesis—and its theoretical rationalization—are currently under way in these laboratories.

In addition to the sign of V_{zz}, the Mössbauer data at 4.2 K also yield a value for the magnitude of the magnetic hyperfine interaction at ^{57}Fe, which can be calculated from the separation of the two outermost peaks of the magnetically split resonance spectrum. Calibration is most readily effected from the observed splitting in metallic iron, for which the magnetic hyperfine field is taken to be 330 kOe at 295 K. The H_{int} values so calculated are included in the data summary of Table I and show that in both the TEP and TMP intercalates the hyperfine field at liquid-helium temperature is identical (within experimental error) with that in unintercalated FeOCl and similar to the values observed in the amine intercalates. From the observed line widths there is no evidence of the presence of more than one distinct hyperfine field at the iron nucleus at 4.2 K. This observation is consistent with the superexchange model of spin correlation in which the long-range magnetic order is assumed to be propagated along the Fe–O–Fe plane (a,c axes) and independent of any interaction across the van der Waals gap.

It is interesting to note, however, as already mentioned above, both the IS and QS parameters of ^{57}Fe in the two intercalates at 4.2 K differ significantly from the corresponding values for unintercalated FeOCl. The present data suggest that these changes in the electron density and charge distribution at the ^{57}Fe nucleus do not affect the magnetic hyperfine interaction within the experimental accuracy of the present experiments.

(d) Intensity Asymmetry of the Mössbauer Spectral Components at $T > T_N$. In FeOCl, the ferric ion occupies an octahedral coordination site with two oxygen ions at 1.964 Å, two further oxygen ions at 2.100 Å, and two chloride ions at 2.368 Å. Although such a bonding environment per se is not expected to lead to significant anisotropy in the vibrational amplitude of the metal atom, the lattice motion due to the relatively weak bonding in the b direction (across the van der Waals layer) may contribute significantly to the intensity asymmetry observed in the Mössbauer spectra. The situation in FeOCl is simplified by the fact that the mm point symmetry of the Fe^{3+} site requires that the principal components of the EFG tensor must be parallel to the a, b, and c crystallographic axes. Moreover, the bladelike habit of the crystals is such that the crystallographic b axis is perpendicular to the plane of the platelet. Thus, even for a finely subdivided, nominally randomly oriented sample consisting of microcrystalline particles, preferential sample orientation may make a nonnegligible contribution to the observed spectral intensity asymmetry. However, these two contributions to the intensity ratio observed in the Mössbauer spectra can be distinguished, since the bonding anisotropy effect will be temperature dependent while

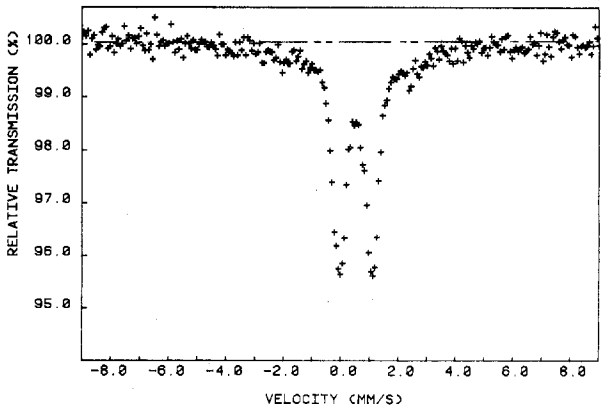

Figure 8. Mössbauer spectrum (^{57}Fe) for the TMP intercalate at 78 K. The broken line is the base line corrected for geometric effects. The absorption due to the magnetically ordered iron atoms is readily discernible.

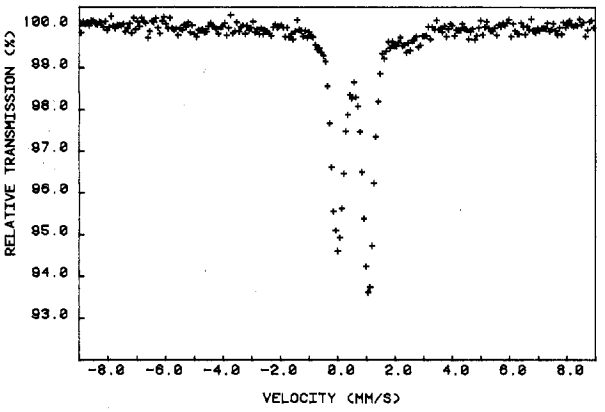

Figure 9. Mössbauer spectrum (^{57}Fe) for the TMP intercalate at 100 K.

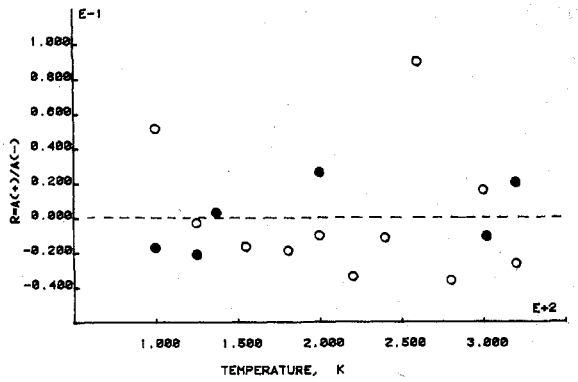

Figure 10. Temperature dependence of the area ratio, R, for FeOCl (filled circles) and the TMP intercalate (open circles). The temperature-independent part of R, assumed to be due to preferential crystal orientation with respect to the γ-ray axis, has been subtracted from the experimental data.

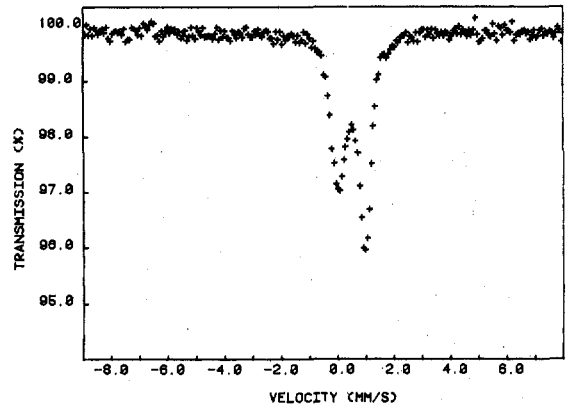

Figure 11. Mössbauer spectrum (^{57}Fe) for the TEP intercalate at 150 K.

the crystal orientation effect is temperature independent.

Mössbauer spectra of the TMP intercalate at 78 and 100 K are shown in Figures 8 and 9. At liquid-nitrogen temperature the two intensity maxima are essentially identical, whereas at the higher temperature there is a sudden onset of an intensity asymmetry, with the more positive velocity peak, $A(+)$, having the larger intensity. The area ratio $R = A(+)/A(-)$ at $T \geq 100$ K for the TMP intercalate is essentially temperature independent, and this temperature-independent part of R is represented by the filled circles in Figure 10. Moreover, in Figure 8 it should be noted that there is a significant resonance absorption noticeable in the data over the velocity range $\sim -3 < v < 3$ mm s^{-1}, as indicated by the departure of the data in the wings of the resonance curve from the flat base line (indicated by the dotted line in Figure 8).

Similar results are noted for the TEP intercalate, for which the resonance spectra at 155 and 300 K are shown in Figures 11 and 12, and the temperature-independent part of R is shown in Figure 10 by the open circles. The absence of a temperature-dependent intensity asymmetry in these samples at temperatures above the magnetic ordering temperature indicates that the iron atom motion parallel and perpendicular to the van der Waals layer plane is essentially isotropic; that is, $\langle x_a^2 \rangle \approx \langle x_b^2 \rangle$, where a and b refer to the crystallographic axes of FeOCl.

These data can be understood on the basis of the following model. The intensity asymmetry noted in the Mössbauer spectra above ~ 100 K arises from the near superposition of two quadrupole-split doublets, having nearly identical isomer shifts and quadrupole splittings, with the two positive velocity components located at the same velocity and the two negative

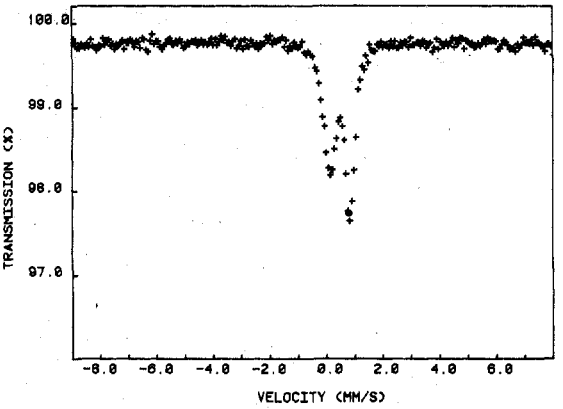

Figure 12. Mössbauer spectrum (^{57}Fe) for the TEP intercalate at 300 K.

velocity components displaced from each other by twice the difference in the isomer shifts of the two iron atoms. This assumption is consistent with the observation that the line width (fwhm) of the negative velocity peak is ~ 0.15–0.3 mm s^{-1} larger than the positive velocity peak line width.

As the temperature is lowered, one of the two types of iron atoms orders before the other one, and, in particular, at 78 K, one type of iron atom shows a magnetic hyperfine splitting which is, however, unresolved and only observed as a departure of the data from a simple two-Lorentzian fit as discussed above (see Figure 8). The other type of iron atom is still in a paramagnetic (not magnetically ordered) state at 78 K. From detailed analysis of the data at 78 K it is noted that about one-sixth of the total area is due to magnetically ordered iron atoms while the remainder of the iron atoms occupy paramagnetic sites. Since the magnetic ordering temperature of unintercalated FeOCl has been shown by several investigators[11,12] to be $\sim 90 \pm 2$ K (although Kostiner and Steger[23] cite a value of 68 ± 2 K[24]), it may be inferred that these iron atoms which have a "guest" molecule near neighbor have higher T_N than iron atoms further removed from the site of the "guest" molecule (possibly of particular significance in this regard is the location within the lattice of the electron density due to the lone pair of the intercalant). A concomitant conclusion is that the iron atoms not in the immediate vicinity of the intercalant have a T_N which is *lower* than that observed in the unintercalated lattice. The difference in T_N between the two types of iron atoms may be as small as ~ 15 K, and it seems clear from the present data that minor differences in the electron density or the shape of the charge distribution around the iron atom can have an observable influence on the magnetic ordering temperature, although they are too small to be observable in the lattice dynamical (temperature-dependent recoil-free fraction) data. A serious weakness of this model is that it would require a mechanism for spin–spin correlation between about one-sixth of the iron atoms in the FeOCl matrix, leaving the other five-sixths of the iron atoms still in a paramagnetic state. Despite the multiple superexchange pathways (via the oxygen atoms) which exist in this structure, it is not clear exactly how this ordering of one type of iron atom can occur without the ordering of all of the iron atom spins. Further detailed studies related to the intercalant structure and the Fe:G ratio as these relate to T_N are currently under way in these laboratories.[24]

(23) Kostiner, E.; Steger, J. *J. Solid State Chem.* **1971**, *3*, 273.
(24) There is considerable reason to suspect (Halbert, T. J., private communication), that T_N for FeOCl is sensitively dependent on the method of preparation and the subsequent purification procedures employed by different investigators. Of importance for the present discussion is the observation that FeOCl used in the preparation of the TEP and TMP intercalates has a reproducible T_N of 90 ± 2 K, as discussed in the text.

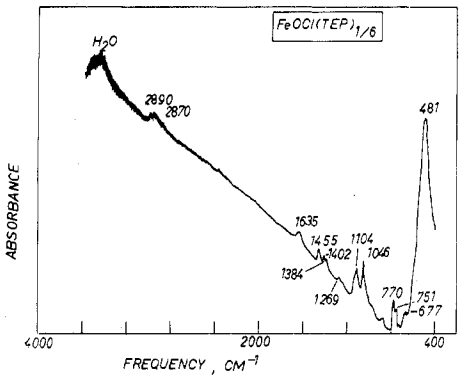

Figure 13. Fourier-transform infrared spectrum of the TMP intercalate at room temperature. Sample concentration is ~0.36% by weight in KBr.

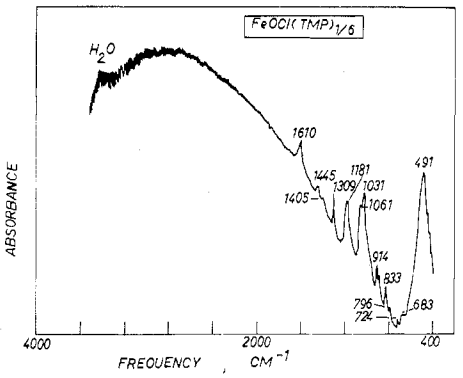

Figure 14. Fourier-transform infrared spectrum of the TEP intercalate at room temperature. Sample concentration is ~0.33% by weight ion KBr.

(e) Infrared Spectra of FeOCl Intercalates. The room-temperature infrared and Raman spectra of trimethyl phosphite have been reported by Nyquist,[25] and the assignment of the vibrational spectrum of triethylphosphine has been discussed by Green[26] in the light of an earlier study of Kaesz and Stone.[27] The room-temperature infrared spectra of the TMP and TEP intercalates of FeOCl are shown in Figures 13 and 14.

There are several features of these spectra which can be related to the question of the interaction of the intercalant with the host matrix. In the TMP intercalate, the strong modes observed at 2955 cm^{-1} (vapor), 2949 and 2939 cm^{-1} (10% CCl_4 solution), and 2937 cm^{-1} (neat liquid) are essentially absent (Figure 13). These modes, which have been assigned by Nyquist to asymmetric and symmetric C–H stretches of the methyl group, appear to be completely inhibited in the lattice. The methyl group asymmetric deformation observed at 1465 cm^{-1} (vapor) to 1459 cm^{-1} (liquid) appears as a broad band centered at ~1445 cm^{-1} in the intercalate. The CH_3 out-of-plane and in-plane rocking modes at 1181 cm^{-1} are unshifted in the intercalate, but their intensity is very much enhanced relative to the asymmetric $P(-O-C)_3$ mode at 1032 cm^{-1}, which is also unshifted in the intercalate. The two modes at 762 and 734 cm^{-1} (vapor), assigned by Nyquist to $P(-O-)_3$ modes, are shifted in the intercalate. Whether these bands are those observed at 796 (blue shift by 34 cm^{-1}) and 724 cm^{-1} (red shift by 8 cm^{-1}) is not unambiguously clear from the present data. Finally it should be noted that in the TMP intercalate there is a strong band observed at 1309 cm^{-1} which is observed neither in FeOCl nor in the neat phosphite and does not appear to be a combination band. The origin of this spectral feature remains to be identified.

In the TEP intercalate infrared spectrum (Figure 14) the spectral changes are similar to those noted above. The CH_3 and CH_2 asymmetric stretches observed at 2900–2998 cm^{-1} in the neat phosphine are extremely weak in the intercalate spectrum. The CH_3 asymmetric deformation at 1423 cm^{-1} is not observed in the intercalate, but instead there are moderately strong bands at 1455 and 1402 cm^{-1} which may represent a red and blue shifted component of this mode. The CH_2 symmetric deformation (scissor mode) at 1380 cm^{-1} is unshifted in the intercalate, appearing as a weak fracture at 1384 cm^{-1}. Similarly the A mode discussed by Green, appearing at 1043 cm^{-1} in the neat phosphine, is observed as a strong mode at 1046 cm^{-1}, and the CH_2 rocking modes may be shifted by a maximum of about 5 cm^{-1} in the intercalate (770 and 751 cm^{-1}). It is of particular interest to note that the strong asymmetric stretch assigned to the CP moiety at 690 cm^{-1} in the infrared and the 670-cm^{-1} mode, which is medium strong in the IR and strong in the Raman spectra, are considerably shifted in the intercalate. In the region between 740 and 600 cm^{-1}, where the C–P modes are expected to be observed, the only resolvable features are noted at 731 and 677 cm^{-1} in the intercalate at room temperature. When the sample is cooled to ~201 K, the 730-cm^{-1} band remains unchanged, the 677-cm^{-1} band is blue shifted to 684 cm^{-1}, and a new feature appears at 628 cm^{-1} (this latter band may be lost in the strong FeO stretch centered at 481 cm^{-1} in the room-temperature spectrum).

While the detailed study of the temperature-dependent vibrational spectra of these intercalated species is still incompletely explored (and even less well understood), the above data suggest that at room temperature, a number of the fundamental vibrational modes appear unaffected on intercalation, while the modes assigned to the terminal C–H stretches appear to be strongly inhibited. The change in the C–P stretching region observed on sample cooling to $T \lesssim 220$ K again evidences the relatively strong bonding (compared to thermal energies) between the "guest" molecule and the host matrix at low temperatures and points to a direct involvement of the phosphorus atom lone pairs in this interaction as the temperature is reduced.

Acknowledgment. This research was generously supported by the National Science Foundation under Grants DMR 76-00139 and DMR 7808615A1, as well as by a grant from the Center for Computer and Information Services of Rutgers University. The authors are grateful to Professors M. Pasternak and N. B. Koller for numerous helpful discussions relating to data analysis. We are indebted to Dr. D. Saperstein of the Merck Sharpe and Dohme Laboratories, Rahway, NJ, for the Fourier-transform infrared spectroscopy data discussed in the present study and to the time and effort which he generously expended in discussing these spectra with us.

Registry No. FeOCl, 13870-10-5; TMP, 121-45-9; TEP, 554-70-1.

(25) Nyquist, R. A. *Spectrochim. Acta* **1966**, *22*, 1315.
(26) Green, J. H. S. *Spectrochim. Acta, Part A* **1968**, *24A*, 137.
(27) Kaesz, H. D.; Stone, F. G. A. *Spectrochim. Acta* **1959**, *15*, 360. See also: Miller, R. G. J. *Colloq. Spectrosc. Int.* [*Proc.*], *12th* **1965**, 523.